Performance Comparison of Single-Sideband Direct Detection Nyquist-Subcarrier Modulation and OFDM

M. Sezer Erkılınç, *Student Member, IEEE*, Stephan Pachnicke, *Senior Member, IEEE*,
Helmut Griesser, *Member, IEEE*, Benn C. Thomsen, *Member, IEEE*, Polina Bayvel, *Fellow, IEEE, Member, OSA*,
and Robert I. Killey, *Member, IEEE*

Abstract—**Direct detection transceivers offer advantages, including low cost and complexity, in short- and medium-haul links. We carried out studies seeking to identify the signal formats which offer the highest information spectral densities and maximum transmission distances for direct detection links. The performance of two spectrally efficient optical signal formats, single-sideband (SSB) Nyquist pulse-shaped subcarrier modulation (SCM) and SSB orthogonal frequency-division multiplexing (OFDM), are compared by means of simulations. The comparison is performed for a range of wavelength-division multiplexing (WDM) net information spectral densities up to 2.0 b/s/Hz by varying the signal bandwidth, modulation cardinality, and WDM channel spacing. The signal formats' tolerance to signal–signal beating interference, resulting from square-law detection, is investigated, and the Nyquist-SCM format is found to suffer lower penalties from this nonlinearity at high information spectral densities. In 7 × 28 Gb/s WDM transmission at 2.0 b/s/Hz (with electronic pre-distortion and EDFA-only amplification), Nyquist-SCM signals can be transmitted over distances of up to 720 km of standard SMF in comparison to a maximum of 320 km with the OFDM signal format.**

Index Terms—**Digital signal processing, direct detection, electronic pre-distortion, Nyquist pulse shaping, optical communication, orthogonal frequency division multiplexing, signal–signal beating interference, subcarrier modulation, wavelength division multiplexing.**

I. INTRODUCTION

THE demand for high bit-rate transmission using cost-effective solutions is continuously increasing, especially in short and medium reach optical links. In order to meet this demand, multilevel modulation techniques achieving spectrally-efficient transmission are attractive and have started to be utilized in the last decade [1], [2]. The highest information spectral densities (ISDs) have been achieved using polarization multiplexing and coherent detection, enabling full recovery of the optical field, and such systems have become the standard in long and ultra-long transmission links. However, due to their potentially lower complexity and cost, single polarization and direct detection transceivers may be an attractive solution for shorter distances, such as in short reach optical links, e.g., data centers and interconnect applications, typically up to 10 km, and medium reach optical links, e.g., access and wireless back-haul links as well as metro and regional distances, typically up to 800 km. The cost could be significantly reduced due to the lower number of optical components required, relaxation of the laser linewidth requirements, and the lower complexity of digital signal processing (DSP) at the receiver. A key question then is, what signal formats offer the highest ISDs and maximum transmission distances in direct detection links.

A variety of formats have been proposed to achieve high ISD, including pulse amplitude modulation (PAM), optical duobinary (ODB), subcarrier modulation (SCM) (e.g., Nyquist-subcarrier modulation (Nyquist-SCM) and orthogonal frequency division multiplexing (OFDM)) and carrierless amplitude phase (CAP) modulation. PAM is the simplest format but suffers from low receiver sensitivity [3]. ODB transmission has been demonstrated at ISDs of 0.8 b/s/Hz [4] and 1 b/s/Hz [5], but it is fundamentally limited to 1 b/s/Hz. Hence, we focus on single sideband (SSB) SCM formats (Nyquist-SCM and OFDM) with quadrature amplitude modulation (QAM) of the RF-subcarrier(s), which are detected by beating with the optical carrier. They enable ISDs greater than 1 b/s/Hz with a good optical signal-to-noise ratio (OSNR) performance. Unfortunately, the receiver sensitivity performance of direct detection SCM formats degrades due to the nonlinear square-law detection, resulting in signal-signal beating interference (SSBI), sometimes referred to as intermodulation distortion.

In this paper, we investigate the transmission performance of SSB Nyquist pulse-shaped SCM and SSB OFDM using direct detection in the presence of SSBI. Their tolerance to SSBI is directly compared by varying the spectral guard band between the optical carrier and sideband in both single channel and wavelength division multiplexing (WDM) system architecture. We consider the use of electronic pre-distortion (EPD), sometimes referred to as electronic dispersion pre-compensation to mitigate the dispersion accumulated along the fibre link, for both formats. In the case of OFDM, bit loading is applied to minimize the penalty due to the SSBI. Their performance in back-to-back operation, and in transmission over standard single mode fibre (SMF) links (both single channel and WDM) is assessed by simulations. The comparison is performed at a symbol rate of

Fig. 1. System architecture for single channel (top) and WDM system (bottom).

Fig. 2. Spectrum of detected SCM signals (a) non-overlapping and (b) overlapping case. Total bandwidth (B_t) is equal to $2B_s - B_{ov}$ where B_s is the signal bandwidth, and B_{ov} is the overlapping bandwidth between the signal and signal–signal beating products. B_g is the spectral guard band between the optical carrier and sideband.

7 GBaud with QAM modulation to achieve per-channel bit rates of up to 28 Gb/s and, WDM net ISDs of up to 2.0 b/s/Hz assuming the use of hard-decision forward error correction (HD-FEC).

II. DESCRIPTION OF NYQUIST-SCM AND OFDM TECHNIQUES

The direct detection system architecture considered in this paper is shown in Fig. 1. In the direct detection SCM technique, a single or multiple subcarrier(s), also referred to as RF-subcarrier(s), is/are used to transmit data over a fibre link. High-order modulation is achieved by applying QAM to the subcarrier(s) and using linear optical field modulation. At the receiver, the channel of interest is optically demultiplexed by an optical band-pass filter (OBPF) and optical-to-electrical conversion is achieved by a single-ended photodiode, beating between the optical carrier and the sideband during the square-law photodetection. Then, the electrical signal is digitized using a single ADC, as depicted in Fig. 1.

However, the photodetection process generates unwanted additional components, referred to as signal-signal beating products, which interfere with the desired signal, referred to as carrier-signal beating products. This effect is termed as SSBI. One approach to reduce the associated performance degradation is the use of SSBI estimation/cancellation. There are some proposed estimation/cancellation techniques to reduce this interference. However, they result in degradation in receiver sensitivity due to high carrier-to-signal power ratio (CSPR) [6], [7], increased DSP complexity [8], [9], optical complexity or overheads [10], [11]. An alternative approach is to use a spectral guard band between the sideband and the optical carrier with bandwidth, B_g (see Fig. 2). Since the signal–signal beating products bandwidth is equal to the signal bandwidth (B_s), the guard band bandwidth must be set such that $B_g \geq B_s$ to avoid any spectral overlap between the carrier-signal and signal–signal beating products. However, this results in a reduction of the ISD by a factor of two and inefficient use of the available bandwidth of RF components used in the system [12]. Alternatively, the bandwidth of the guard band may be set to a lower value, i.e.,
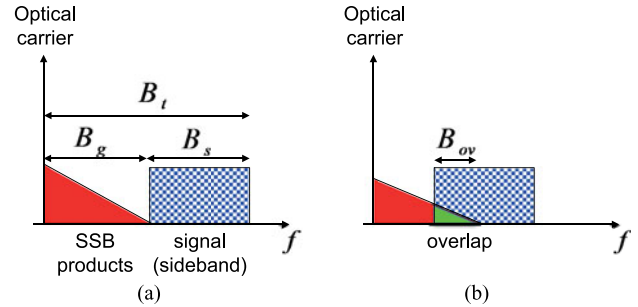
$B_g < B_s$, to achieve the desired ISD/OSNR penalty trade-off depending on the overlap between the sideband and signal–signal beating products [13]. In the following, to quantify the amount of overlap between the sideband and signal–signal beating products, we use the overlapping ratio parameter, defined as the ratio of the overlapping bandwidth (B_{ov}) and B_s, as depicted in Fig. 2(b).

In this paper, we considered two types of spectrally-efficient direct detection SCM formats: SSB OFDM, and SSB single SCM with Nyquist pulse shaping. OFDM is widely used in digital communication systems to achieve high ISD [14]. It is a multi-SCM technique in which a data stream is encoded onto multiple densely-spaced orthogonal subcarriers in the frequency domain using the inverse discrete Fourier transform. Although it allows increased ISD with a simple receiver structure, the receiver sensitivity is affected by the high peak-to-average power ratio (PAPR) of the signal, caused by high peaks in signal waveform. They occur due to the constructive addition resulting from the phase alignments of the subcarriers [15]. High PAPR results in an increase in the required CSPR, nonlinear distortion, and also the required dynamic range of the DACs/ADCs used in the transceiver, causing increased converter quantization noise. The alternative SCM format we considered, single SCM, in which a QAM signal is electrically modulated onto a single subcarrier, potentially has lower PAPR compared to OFDM since it utilizes only one subcarrier and avoids the problem of constructive addition of multiple subcarriers. The subcarrier frequency (f_{sc}) and roll-off factor of the pulse shaping filter (α) are selected according to the required optical ISD and receiver sensitivity requirements. To maximize the ISD, the RF-subcarrier frequency should be set to a value close to half of the symbol rate, and the pulse shaping filter should have a roll-off factor close to zero. Single-cycle SCM quaternary phase-shift keying (QPSK) and 16-QAM in which f_{sc} was set equal to the symbol rate (f_s), were demonstrated in [16]. In addition to single-cycle, half-cycle ($f_{sc} = f_s/2$) Nyquist-SCM 16-QAM was also demonstrated back-to-back and in transmission over 4 km of standard SMF in [17] to achieve ISD approaching $\log_2(M)/2$ for M-QAM. The very close spacing between the optical carrier and subcarrier is enabled by using Nyquist pulse shaping filters with root raised cosine (RRC) transfer function and α of ≤ 0.4 [18]. For both
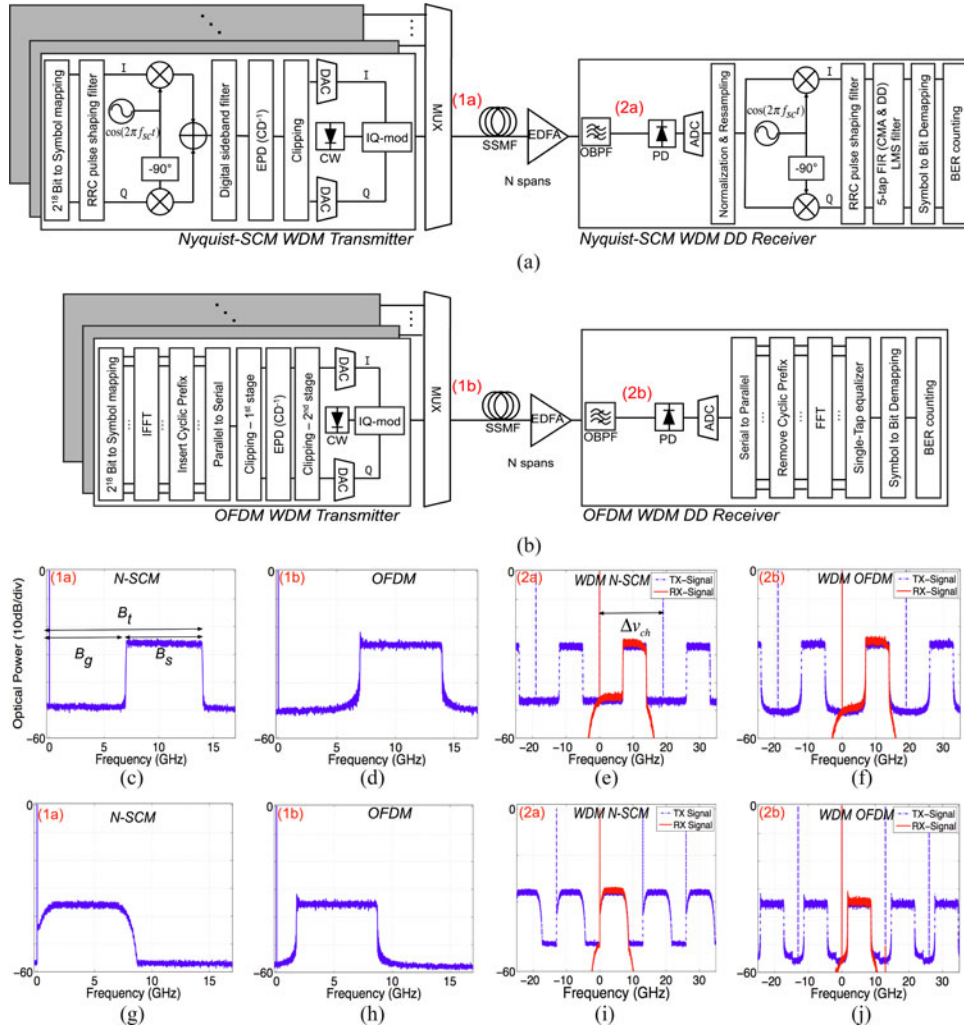
Fig. 3. (a) Nyquist-SCM and (b) OFDM system diagram. Single channel optical spectra for (c) Nyquist-SCM and (d) OFDM signals, and WDM spectra before and after the OBPF for (e) Nyquist-SCM and (f) OFDM signals with a B_t of 14 GHz and a Δv_{ch} of 19 GHz (non-overlapping case). Single channel optical spectra for (g) Nyquist-SCM and (h) OFDM signals, and WDM spectra after the OBPF for (i) Nyquist-SCM and (j) OFDM signals with a B_t of 8.75 GHz and a Δv_{ch} of 13 GHz (overlapping case). Note that frequency scales in optical spectra are relative to the optical carrier frequency of the central channel.

the OFDM and Nyquist-SCM signal formats considered in this study, the ISDs are increased by digitally suppressing one of the sidebands, referred to as SSB signalling, to achieve ISD approaching $\log_2(M)$. The trade-off between α and f_{sc} for SSB single SCM was investigated in [19] and it was shown that a RRC filter roll-off factor of 0.3 with $f_{sc} = 0.75 f_s$ provides a good compromise between the ISD and receiver sensitivity. A transceiver design using these parameters was experimentally demonstrated to achieve WDM SSB Nyquist pulse-shaped single SCM QPSK transmission over standard SMF links of up to 800 km at an ISD of 1.3 b/s/Hz [19].

In this study, the performance of OFDM and single SCM formats with equivalent ISDs are compared; the symbol rate of the signals is kept constant at 7 GBaud, with gross bit-rates per channel of 14 and 28 Gb/s, respectively. The ISD is varied by varying the guard band (B_g) between the optical carrier and the sideband (hence changing the overlapping ratio parameter, B_{ov}/B_s), and the WDM channel spacing (Δv_{ch}). The performance of the signal formats is compared in terms of the required

optical signal-to-noise ratio (OSNR) in back-to-back operation, and the maximum transmission distance over standard SMF links (including the effects of EDFA noise, fibre dispersion and nonlinearity). No digital or optical SSBI estimation/cancellation is carried out to avoid significant additional transceiver complexity.

III. NYQUIST-SCM AND OFDM SYSTEM MODELS

The system diagrams for WDM Nyquist-SCM and OFDM signal generation, transmission and detection, that were modelled in MATLAB, are shown in Fig. 3(a) and (b) with the single channel and WDM optical spectra for the cases of channel bandwidths (B_t) of 14 and 8.75 GHz. Transmission simulations using the split-step Fourier method to solve the nonlinear Schrödinger equation were carried out for a range of values of B_g and consequently, B_t and Δv_{ch}. For the Nyquist-SCM simulations, a 7 GBaud conventional QPSK/16-QAM signal was generated using two/four de-correlated 2^{18} de Bruijn bit

sequences. Subsequently, a pair of 256-tap RRC filters with a stop-band attenuation of 40 dB were applied to the in-phase (I) and quadrature (Q) components separately to achieve Nyquist pulse shaping as shown in Fig. 3(a). Then, the Nyquist pulse-shaped signals were up-converted to the subcarrier frequency and added to each other to obtain a double sideband Nyquist-SCM QAM signal. Following this, a sideband filter was applied digitally to obtain the SSB signal. In back-to-back operation, there was no need to apply clipping for the Nyquist-SCM signal since its PAPR value was equal to 7.8 dB which was sufficiently low. The PAPR of a complex signal is defined as

$$\text{PAPR} = \frac{\max[s(t)s^*(t)]}{E[s(t)s^*(t)]} \text{ and } \text{PAPR}_{\text{dB}} = 10\log_{10}(\text{PAPR}) \quad (1)$$

where $s(t)$ is the complex signal, t is the time index and $E[s(t)s^*(t)]$ is the expected value of the signal power. Note that PAPR value was found to be almost the same for both QPSK and 16-QAM. Finally, EPD [20], [21] and clipping [22] were applied in transmitter DSP to mitigate the chromatic dispersion accumulated at the targeted distance with a minimum penalty. The clipped signal can be formalized as

$$s_{\text{clipped}}(t) = \begin{cases} s(t), & \text{if } |s(t)| \leq A \\ Ae^{j\arg\{s(t)\}}, & \text{if } |s(t)| > A \end{cases} \quad (2)$$

where $s_{\text{clipped}}(t)$ represents the clipped signal, A is the maximum amplitude value after clipping and $\arg\{s(t)\}$ is the phase of $s(t)$. The clipping ratio is commonly defined as the ratio of the maximum to the average output power [23].

The OFDM signal generation is shown in Fig. 3(b). 128 data subcarriers were first modulated, and multiplexed using a 256-point inverse fast Fourier transform (IFFT) (an oversampling ratio of 2). Then, a 2% cyclic prefix (CP) was added as a guard band to avoid the inter-symbol interference due to filter delays introduced by electrical and optical filters in the system. Unlike Nyquist-SCM, clipping (first-stage) was applied to back-to-back OFDM signal (prior to EPD) to optimize its performance. Its PAPR was reduced from 14.8 to 11.3 dB. After clipping, similar to the Nyquist-SCM signal, EPD and clipping (second-stage) were applied to the OFDM signal in the frequency domain to mitigate the dispersion with a minimum penalty (rather than using a longer CP) in order to operate at the same ISD as the Nyquist-SCM signal. The resolution of the DACs operating at 28 GSa/s was assumed to be 5 bits for both Nyquist-SCM and OFDM systems which was sufficient to avoid significant penalties (≤ 0.5 dB) due to the quantization noise. It is expected that the use of high sampling rate DACs and ADCs will be acceptable in future low-cost systems, as the performance of silicon complementary metal oxide semiconductor (CMOS) technology continues to increase, and the cost and power consumption reduce. The electrical bandwidth of the transmitter and receiver were emulated using fifth-order Bessel low-pass filters (LPFs) with an optimized bandwidth of 0.8 f_s. The optical carriers were added at the IQ-modulators being biased close to their quadrature points to achieve approximately linear mapping from the electrical to the optical domain with the desired optical carrier power. To model WDM transmission, all

seven WDM channels each carrying 28 Gb/s SSB Nyquist-SCM 16-QAM or the equivalent adaptively modulated OFDM signal were decorrelated by more than 17 ns (one symbol period is 140 ps).

The total bandwidth of a single channel (B_t) is the sum of B_g and B_s as shown in Figs. 2(a) and 3(c). To compare the ISD of modulation techniques fairly, B_t was kept the same for both techniques. When the overlapping ratio was equal to 0, B_s was set to 7 GHz at 7 GBaud, as can be seen in Fig. 3(c) and (d). In the case of non-zero overlapping ratio ($B_{ov} > 0$ GHz so $B_t < 14$ GHz), the SSBI decreases towards higher frequencies, so that the subcarriers close to the optical carrier are more significantly affected than those further away from the carrier. If the same constellation scheme is used for all subcarriers, the error probability is severely affected since it is dominated by the subcarriers with the highest distortion. To overcome this issue, and consequently, optimize the system performance, each subcarrier can be modulated with an optimally chosen format cardinality (also termed bit loading), so that similar bit error probabilities are experienced by all the subchannels. This bit loading can be adapted, according to the frequency dependent signal-to-noise ratio (SNR), and this technique is referred to as adaptively modulated OFDM. In the system considered in this paper, bit loading was applied depending on the SNR of each subcarrier using a "water-filling" approach with M-QAM modulation used for M bits/symbol [24]. For the bit loading, the Levin–Campello algorithm was utilized since it provides an optimum discrete bit distribution (finite granularity) assuming the information granularity is the same for all subchannels which is usually the case [25]. The bits were allocated to the subcarriers by comparing the SNR threshold values for conventional modulation formats, e.g., BPSK, QPSK etc., and their received SNR values which were obtained from the receiver. Since their received SNR values also depend on the CSPR, the optimum bit allocation was found by applying an exhaustive search for the CSPR value to achieve the best OSNR performance. For instance, to achieve a bit-rate of 28 Gb/s (requiring an average number of bits/symbol of 4 for the 7 GBaud signal), as the subcarriers overlapping with the signal–signal beating products had lower SNR values than the non-overlapping ones (see Fig. 4(a)), they were allocated lower numbers of bits per symbol (0, 1, 2 and 3 bits/sym). On the other hand, the subcarriers that did not overlap with the beating products were allocated with higher bits/symbol (4, 5 and 6 bits/sym) depending on their SNR values as shown in Fig. 4(b). The power was kept uniform across the subcarriers. The bit loading algorithm stopped when the desired bit-rate was achieved. Although bit loading significantly increases the receiver sensitivity compared to uniform modulation, it requires a feedback from the receiver to the transmitter to obtain the SNR values of each subcarrier [25], [26].

SNR, bit allocation and BER values per subcarrier at an OSNR of 26 dB, a CSPR of 13 dB and a B_t of 8.75 GHz are shown in Fig. 4. At this B_t, 97 subcarriers (first subcarrier is the closest one to the optical carrier) overlapped with the signal–signal beating products. Since the distortion caused by the SSBI gradually decreased towards the higher frequencies due to the superposition of the subcarriers, each subcarrier was
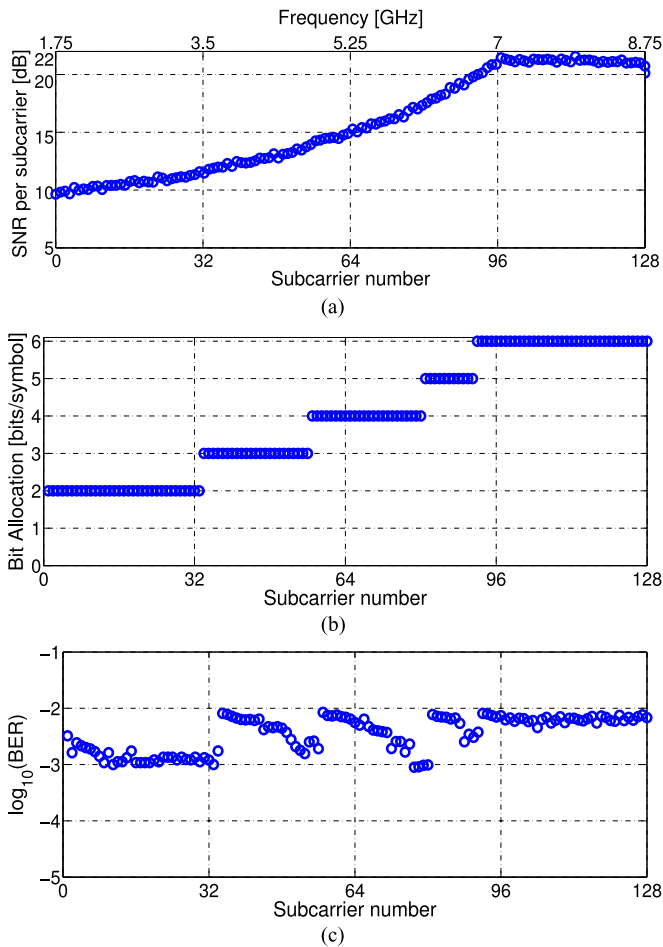
Fig. 4. OFDM bit loading for the case of a CSPR of 13 dB, an OSNR of 26 dB, and a B_t of 8.75 GHz at the HD-FEC limit. (a) SNR in decibel per subcarrier, (b) bit allocation per subcarrier to achieve 28 Gb/s and (c) BER values per subcarrier.

TABLE I
OPTICAL BW AND ISD VALUES USED IN THE SIMULATIONS

B_t (GHz)	B_s (GHz)	B_g (GHz)	B_{ov} (GHz)	Δv_{ch} (GHz)	Net ISD (b/s/Hz)
14	7	7	0	19	1.37
8.75	7	1.75	5.25	13	2.0

The transmission link considered in the simulations was uncompensated standard SMF and the fibre parameters α, D, γ, Erbium-doped fibre amplifier (EDFA) noise figure and span length were chosen as 0.2 dB/km, 16.8 ps/(nm·km), 1.2 W^{-1} km^{-1}, 5 dB and 80 km, respectively. The EDFA was set to compensate the fibre loss over each span which had 16 dB attenuation. All amplified spontaneous emission (ASE) noise generated by the EDFAs was added inline to model nonlinear signal-ASE beating noise interaction. The single channel and WDM signal transmission in the fibre was modelled using the symmetric split-step Fourier method [29] and the step sizes were empirically chosen as 1 and 0.4 km, respectively at a bandwidth of approximately 200 GHz.

A third-order super-Gaussian OBPF with a bandwidth of 17 GHz (Δv_{ch} = 19 GHz) and 11 GHz (Δv_{ch} = 13 GHz) was utilized to demultiplex the central WDM channel for B_t = 14 and 8.75 GHz, respectively. Then, the filtered channel was detected by a single-ended photodiode with a responsivity of 1 A/W. The resolution and sampling rate of the ADC were assumed to be 5-bit and 28 GSa/s, respectively. The DACs/ADC resolution and the bandwidth of the Bessel LPFs for both modulation formats were chosen such that the implementation penalty was kept within 1 dB for both single channel and WDM transmission. After the detection, the normalized Nyquist-SCM signal was split into two branches and down-converted to I and Q baseband signals. Following this, a pair of matched RRC filters (α = 0.3) was applied to the baseband signals. For optimum sampling, a 5-tap equalizer using least mean squares (LMS) adaptation was applied as shown in Fig. 3(a). The equalizer first utilized the constant modulus algorithm (CMA) as a cost function to update the filter taps for fast convergence and then, switched to decision directed LMS.

In the OFDM case, the digitized detected signal was first converted from serial to parallel, and consequently, the CP was removed from the received signal. Note that no symbol/frame timing synchronization algorithm was applied in our OFDM simulation model for simplicity since the sampling rate of DACs and ADC kept the same. Following this, a 256-point FFT was applied and the channel estimation was performed using a single-tap equalizer to cancel the phase errors and distortions incurred along the transmission path as shown in Fig. 3(b). Training symbols have the same data sequence compared to the data used. They were inserted periodically, every 63 data symbols leading to a 1% overhead, a technique also referred to as block-type channel estimation. The estimation was based on a least-square method so that the coefficients of the single-tap equalizer were derived by comparing the received training symbols with the transmitted ones [30]. To improve the channel estimation performance, a polynomial fit was applied to the derived coefficients.

distorted by different amount of SSBI as shown in Fig. 4(a). The subcarriers that were distorted severely (57 subcarriers) were allocated with less than 4 bits per symbol. The ones that manage to maintain high SNR or do not even overlap with the beating products were allocated with the highest possible bits per symbol in order to achieve the desired bit-rate, that is 28 Gb/s. The BER for each subcarrier varied between ∼1×10^{-3} and 8×10^{-3}. For the best receiver sensitivity performance, BER on each subcarrier should be the same. To equalize BER on each subcarrier, power loading in addition to the bit loading can be also applied instead of allocating the power equally across subcarriers. Nevertheless, at the same bit-rate, the system performance that utilizes power-and-bit loading is not significantly different than systems utilizing only bit loading [26]–[28].

For the case of the Nyquist-SCM system, α was varied from 0 to 0.3 and f_{sc} was adjusted accordingly whilst ensuring that Nyquist-SCM and OFDM signals had equal B_t values as shown in Fig. 3(e) and (f). Table I shows the optical bandwidth (BW) and ISD values considered in the simulations. In both cases, Δv_{ch} was chosen such that there was negligible linear crosstalk penalty between the channels and net ISD is calculated assuming 16-QAM and a 7% HD-FEC overhead.
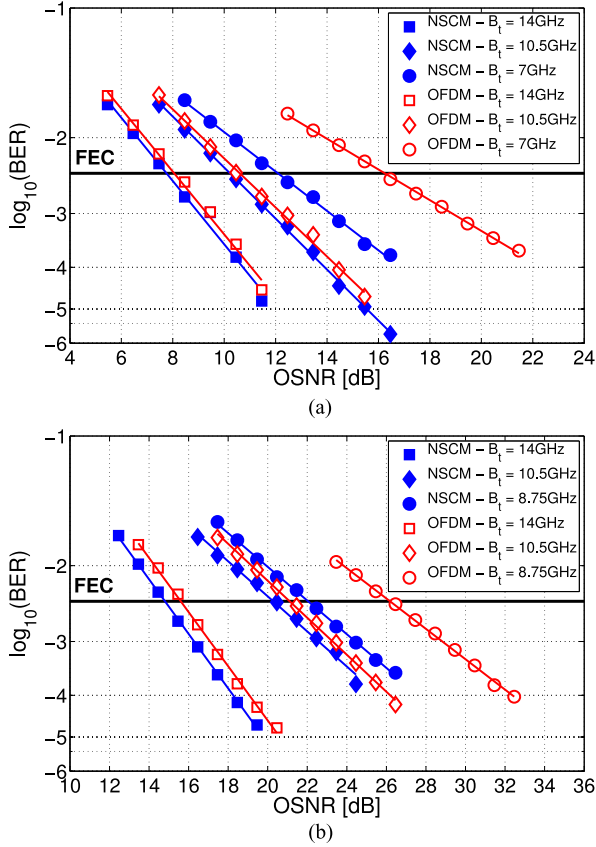
Fig. 5. Back-to-back BER with respect to OSNR with different values of signal bandwidth (B_t) for (a) Nyquist-SCM QPSK and the equivalent adaptively modulated OFDM signals at 14 Gb/s and (b) Nyquist-SCM 16-QAM and the equivalent adaptively modulated OFDM signals at 28 Gb/s.

Fig. 6. Required OSNR with respect to B_t at the HD-FEC limit for Nyquist-SCM QPSK/16-QAM and the equivalent adaptively modulated OFDM signals.

Finally, the received signal was multiplied with the inverse of the estimated channel response to restore the transmitted signal. After equalization, the symbol-to-bit demapping was performed and BER was calculated by counting the errors using 2^{18} bits in both setups. The simulation results are discussed in Section IV.

IV. RESULTS AND DISCUSSIONS

A. Back-to-back

First, back-to-back single channel Nyquist-SCM QPSK/16-QAM and the equivalent adaptively modulated OFDM signals were simulated to determine the receiver sensitivities as shown in Fig. 5. Then, at the HD-FEC limit assuming 7% overhead, the signals were compared at different values of signal bandwidth (B_t), presented in Fig. 6. Note that, no bit-loading was applied for OFDM signal and α was set to 0 for Nyquist-SCM signal when B_{ov} was set to 0. However, with B_t set to less than 14 GHz, α for the Nyquist-SCM signal was relaxed from 0 to 0.3 to achieve a better OSNR performance through increasing its tolerance to SSBI due to averaging the distortion across the signal bandwidth, and reducing its PAPR while adjusting the RF-subcarrier frequency to keep B_t and the ISDs identical to those of the equivalent adaptively modulated OFDM signal. When Nyquist-SCM QPSK is used at a B_t of 14 GHz, the required
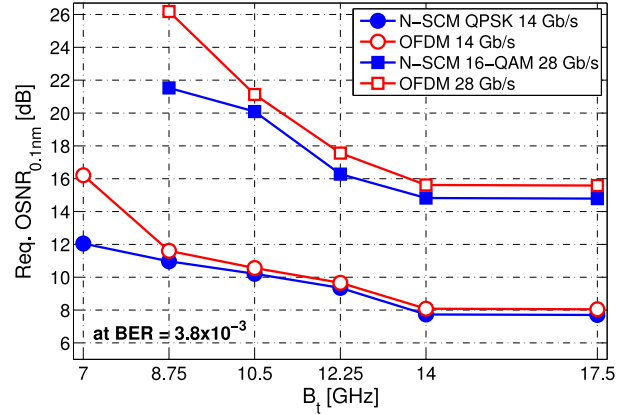
OSNR for Nyquist-SCM is very similar to (approximately 0.8 dB lower than) the equivalent OFDM signal. This performance difference is due to the higher PAPR value of the OFDM signal. With the PAPR of the OFDM signal optimized (by clipping and minimizing the required OSNR) for a 5-bit DAC resolution, its value is still 3.3 dB higher than the PAPR of the Nyquist-SCM signal, calculated using Eq. 1. This difference leads to a higher required optical carrier power to avoid any clipping upon photodetection for the OFDM signal, and hence, the higher required OSNR.

It was found that the performance difference between Nyquist-SCM and OFDM signals at $B_t \geq 8.75$ GHz does not differ significantly until the highest ISD is reached. However, when B_t is less than 8.75 GHz, the required OSNR values for the two signal formats diverge significantly. The Nyquist-SCM format required an OSNR of 12.0 dB at $B_t = 7$ GHz, while the corresponding value for the OFDM signal was found to be 16.1 dB, 4 dB higher than Nyquist-SCM signal (see Fig. 6). When the Nyquist-SCM modulation format was switched from QPSK to 16-QAM (and the bit distribution on the OFDM subcarriers also increased to achieve equivalent ISD values), they had similar OSNR requirements for $B_t \geq 10.5$ GHz. However, at $B_t = 8.75$ GHz, the required OSNR difference between Nyquist-SCM and OFDM signals became again approximately 4 dB. With B_t set to 7 GHz, at which point the gross ISD, 4 b/s/Hz, is close to $\log_2(\mathrm{M})$, neither system was able to achieve the HD-FEC limit BER of 3.8×10^{-3}.

The performance difference between the two formats can be explained by two reasons: 1) Nyquist SCM signal averages the distortion due to the SSBI in the entire signal bandwidth whereas the subcarriers in OFDM signal overlapping with the beating interference are severely affected even though they are modulated adaptively. 2) The Nyquist-SCM signal format has lower PAPR than the OFDM format which reduces the required CSPR value, and hence, the required OSNR for optimum detection. It is worth noting that the slope of the BER versus OSNR curves for QPSK/16-QAM case in Fig. 5 changes when B_t is less than 8.75/10.5 GHz due to the SSBI.

In direct detection systems, optimizing the CSPR is essential to achieve a trade-off between signal-ASE beating noise and SSBI. When $B_t = 14$ GHz, at the OSNR values giving a BER of 3.8×10^{-3}, the optimum CSPR values for both QPSK and 16-QAM were found to be -5 and 0 dB for Nyquist-SCM and OFDM signal formats, respectively. The difference in CSPR values is explained by the difference in PAPR of the signals after clipping. On the other hand, in the case where the signal overlaps with the signal–signal beating products (i.e., $B_t < 14$ GHz), the carrier-signal beating products have to be large enough compared to the SSBI to be recovered. Thus, the optimum CSPR value increases with reducing B_t. At $B_t = 8.75$ GHz, the optimum CSPR value in the case of 16-QAM was found to increase to 6 and 13 dB for the Nyquist-SCM and OFDM signals, respectively, at the HD-FEC limit. This increase in CSPR directly translates into the penalties in the required OSNR as seen in Figs. 5 and 6.

It should be noted that better performance of Nyquist-SCM at high ISD was also observed in [31]. Single channel vestigial sideband Nyquist-SCM was compared with OFDM in back-to-back and transmission performance over 100 km, although without considering any adaptive bit loading for the OFDM signal or EPD to mitigate the chromatic dispersion.

B. Transmission Results

Following the back-to-back simulations described above, both single channel and seven-channel WDM transmission simulations at 28 Gb/s per channel were carried out. In each case, the WDM channel spacing (Δv_{ch}) was chosen such that a negligible penalty (≤ 0.5 dB) resulted due to linear inter-channel crosstalk. Initially, the signal bandwidth B_t was set to 14 GHz ($B_s = B_g = 7$ GHz so that $B_{ov} = 0$ GHz) and a Δv_{ch} of 19 GHz was chosen (resulting in a net ISD of 1.37 b/s/Hz assuming 7% HD-FEC overhead). Fig. 7(a) shows the range of launch powers at which the pre-FEC BER was $< 3.8 \times 10^{-3}$. Due to the low crosstalk between channels, the transmission performance of single channel and WDM are very similar in the linear regime. However, in the non-linear regime in single channel transmission, the lower maximum launch powers indicate that OFDM is more sensitive to self-phase modulation than Nyquist-SCM. Nyquist-SCM has 2 dB greater margin compared to the OFDM signal. This margin was reduced to 0.8 dB in WDM transmission. At $B_{ov} = 0$ GHz or $B_t = 14$ GHz, the maximum transmission distance of Nyquist-SCM and OFDM signal formats were quite similar, (1880 km versus 1720 km, respectively) which was expected from the result, shown in Fig. 6.

Next, B_t was reduced from 14 to 8.75 GHz and consequently, it was possible to reduce Δv_{ch} from 19 to 13 GHz, resulting in an increase in the net ISD from 1.37 to 2.0 b/s/Hz. The single channel and the WDM transmission results at this ISD are presented in Fig. 7(b). In both single channel and WDM transmission cases, Nyquist-SCM offered a maximum transmission distance approximately two times larger than the OFDM signal. This difference is mainly due to ~ 4 dB difference in the required OSNR observed in back-to-back operation between the Nyquist-SCM and the OFDM formats as shown in Figs. 5(b)
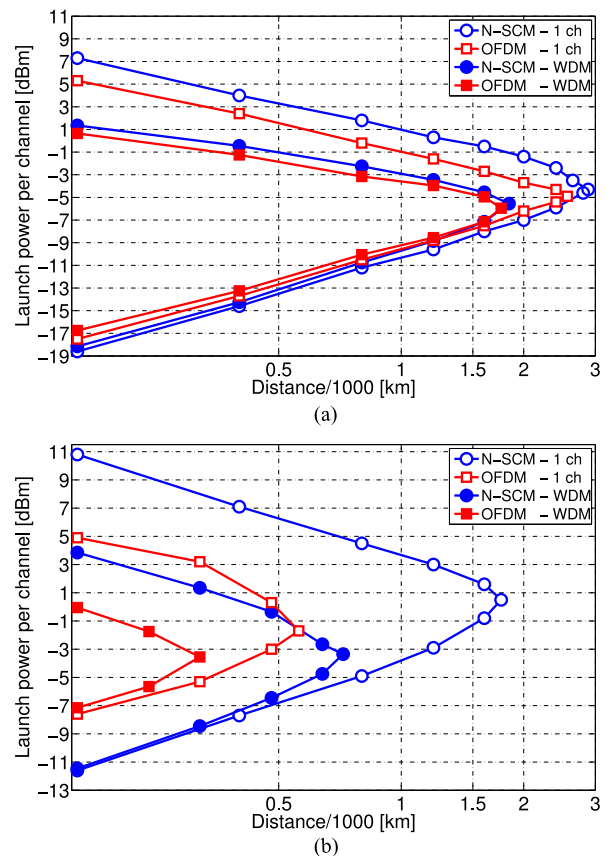

Fig. 7. At BER $= 3.8 \times 10^{-3}$, single channel and WDM transmission performance of 28 Gb/s Nyquist-SCM 16-QAM and the equivalent adaptively modulated OFDM signals at net ISD of (a) 1.37 b/s/Hz ($B_t = 14$ GHz and $\Delta v_{ch} = 19$ GHz) and (b) 2.0 b/s/Hz ($B_t = 8.75$ GHz and $\Delta v_{ch} = 13$ GHz.)
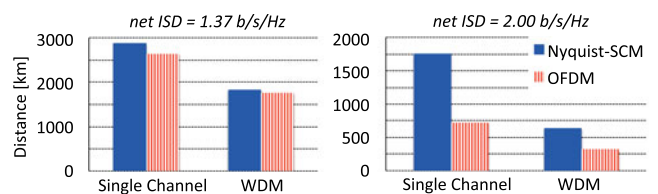

Fig. 8. Maximum transmission distances of single channel and WDM systems for 28 Gb/s Nyquist-SCM and OFDM signals at net ISD of 1.37 b/s/Hz (left) and (b) 2 b/s/Hz (right).

and 6. Accordingly, the WDM Nyquist-SCM signal could be transmitted over distances of up to 720 km of standard SMF whereas the maximum distance with WDM OFDM was just 320 km. The maximum transmission distances of single channel and WDM systems for the Nyquist-SCM 16-QAM and the equivalent adaptively modulated OFDM signals are summarized in Fig. 8.

Further studies are required comparing the performance of Nyquist-SCM with other spectrally-efficient modulation techniques, such as asymmetrically clipped optical OFDM [32], and CAP modulation [3], [33]. Additionally, the use of DSP-based SSBI mitigation methods, which can provide further

performance improvements, needs detailed investigation [8], [13], [34].

V. Summary and Conclusion

We compared two direct detection modulation formats, Nyquist-SCM and OFDM. Both techniques can be used to achieve high ISD (>1 b/s/Hz) transmission. The aim of the comparison in this paper was to assess their tolerance to SSBI at high ISDs as the spectral guard band between the optical carrier and sideband was varied. The roll-off factor of the pulse shaping filter and RF-subcarrier frequency were optimised for the Nyquist-SCM signal whereas bit loading was carried out with the OFDM signal to optimise their tolerance to the SSBI. The performance comparison using QPSK and 16-QAM signalling operating at 7 GBaud per channel for the back-to-back case showed similar required OSNR values for Nyquist-SCM and OFDM signal formats, at the HD-FEC limit of 3.8×10^{-3} when a large spectral guard band ($B_g > 2.75/5.5$ GHz, or $B_t \geq 8.75/10$ GHz for QPSK/16-QAM signal) between the optical carrier and sideband was used. However, the Nyquist-SCM QPSK/16-QAM signal outperformed the equivalent adaptively modulated OFDM signal when the total bandwidth was lower than 8.75/10.5 GHz, leading to, respectively, ∼75%/50% overlap between the signal-signal beating products and sideband. This can be explained by the averaging of the nonlinear distortion caused by the beating interference over the entire signal bandwidth and the lower PAPR of the Nyquist-SCM signal. Following the assessment of back-to-back performance, single channel and WDM transmission performance of the Nyquist-SCM and OFDM signals were compared by simulations at net ISDs of 1.37 b/s/Hz ($B_t = 14$ GHz) and 2.0 b/s/Hz ($B_t = 8.75$ GHz). The results showed that the single channel and WDM system performance of both signal formats were very similar at the lower ISD. However, their performance diverged at 2 b/s/Hz. Seven-channel WDM Nyquist-SCM and OFDM signals can be transmitted over standard SMF distances of up to 720 and 320 km, respectively. Direct detection Nyquist-SCM appears to have a higher tolerance to the SSBI and has the potential to offer the combination of higher ISD, and longer transmission distances with low complexity transceiver design for metro, regional, access and back-haul applications.

Acknowledgment

References

[1] P. Winzer, "High spectral-efficiency optical modulation formats," *J. Lightw. Technol.*, vol. 30, no. 24, pp. 3824–3835, Dec. 2012.

[2] A. H. Gnauck, R. W. Tkach, A. R. Chraplyvy, and T. Li, "High-capacity optical transmission systems," *J. Lightw. Technol.*, vol. 26, no. 9, pp. 1032–1045, May 2008.

[3] J. L. Wei, J. D. Ingham, D. G. Cunningham, R. V. Penty, and I. H. White, "Performance and power dissipation comparisons between 28 Gb/s NRZ, PAM, CAP and optical OFDM systems for data communication

applications," *J. Lightw. Technol.*, vol. 30, no. 20, pp. 3273–3280, Oct. 2012.

[4] E. Pincemin, C. Gosset, N. Boudrioua, A. Tan, D. Grot, and T. Guillossou, "Experimental performance comparison of duobinary and PSBT modulation formats for long-haul 40 Gb/s transmission on G 0.652 fibre," *Opt. Exp.*, vol. 20, no. 27, pp. 28171–28190, 2012.

[5] M. Alfiad and S. Tibuleac, "100G superchannel transmission using 4×28 Gb/s subcarriers on a 25-GHz Grid," *IEEE Photon. Technol. Lett.*, vol. 27, no. 2, pp. 157–160, Jan. 2015.

[6] M. Schuster, S. Randel, C. A. Bunge, S. C. J. Lee, F. Breyer, B. Spinnler, and K. Petermann, "Spectrally efficient compatible single-sideband modulation for OFDM transmission with direct detection," *IEEE Photon. Technol. Lett.*, vol. 20, no. 9, pp. 670–672, May 2008.

[7] Y. Zhang, M. O'Sullivan, and R. Hui, "Theoretical and experimental investigation of compatible SSB modulation for single channel long-distance optical OFDM transmission," *Opt. Exp.*, vol. 18, no. 16, pp. 16751–16764, 2010.

[8] Z. Cao, J. Yu, W. Wang, L. Chen, and Z. Dong, "Direct-detection optical OFDM transmission system without frequency guard band," *IEEE Photon. Technol. Lett.*, vol. 22, no. 11, pp. 736–738, Jun. 2010.

[9] W. R. Peng, X. Wu, K.-M. Feng, V. R. Arbab, B. Shamee, J.-Y. Yang, L. C. Christen, A. E. Willner, and S. Chi, "Spectrally efficient direct-detected OFDM transmission employing an iterative estimation and cancellation technique," *Opt. Exp.*, vol. 17, no. 11, pp. 9099–9111, 2009.

[10] S. A. Nezamalhosseini, L. R. Chen, Q. Zhuge, M. Malekiha, F. Marvasti, and D. V. Plant, "Theoretical and experimental investigation of direct detection optical OFDM transmission using beat interference cancellation receiver," *Opt. Exp.*, vol. 21, no. 13, pp. 15237–15246, 2013.

[11] J. Ma, "Simple signal-to-signal beat interference cancellation receiver based on balanced detection for a single-sideband optical OFDM signal with a reduced guard band," *Opt. Lett.*, vol. 38, no. 21, pp. 4335–4338, 2013.

[12] A. J. Lowery, "Amplified-spontaneous noise limit of optical OFDM lightwave systems," *Opt. Exp.*, vol. 16, no. 2, pp. 860–865, 2008.

[13] W. R. Peng, B. Zhang, K.-M. Feng, X. Wu, A. E. Willner, and S. Chi, "Spectrally efficient direct-detected OFDM transmission incorporating a tunable frequency gap and an iterative detection techniques," *J. Lightw. Technol.*, vol. 27, no. 24, pp. 5723–5735, Dec. 2009.

[14] A. J. Lowery and L. B. Du, "Optical orthogonal division multiplexing for long haul optical communications: A review of the first five years," *Opt. Fiber Technol.*, vol. 17, pp. 421–438, 2011.

[15] J. Armstrong, "OFDM for optical communications," *J. Lightw. Technol.*, vol. 27, no. 3, pp. 189–204, Feb. 2009.

[16] A. O. J. Wiberg, B.-E. Olsson, P. A. Andrekson, "Single cycle subcarrier modulation," presented at the Optical Fiber Communication Conf., San Diego, CA, USA, Mar. 2009, Paper OTuE.1.

[17] A. S. Karar and J. C. Cartledge, "Generation and detection of a 56 Gb/s signal using a DML and half-cycle 16-QAM Nyquist-SCM," *IEEE Photon. Technol. Lett.*, vol. 25, no. 8, pp. 757–760, Apr. 2013.

[18] G. Bosco, A. Carena, V. Curri, P. Poggiolini, and F. Forghieri, "Performance limits of Nyquist-WDM and CO-OFDM in high-Speed PM-QPSK systems," *IEEE Photon. Technol. Lett.*, vol. 22, no. 15, pp. 1129–1131, Aug. 2010.

[19] M. S. Erkılınç, S. Kilmurray, R. Maher, M. Paskov, R. Bouziane, S. Pachnicke, H. Griesser, B. C. Thomsen, P. Bayvel, and R. I. Killey, "Nyquist-shaped dispersion-precompensated subcarrier modulation with direct detection for spectrally-efficient WDM transmission," *Opt. Exp.*, vol. 22, no. 8, pp. 9420–9431, 2014.

[20] R. I. Killey, P. M. Watts, V. Mikhailov, M. Glick, and P. Bayvel, "Electronic dispersion compensation by signal predistortion using digital processing and a dual-drive Mach–Zehnder modulator," *IEEE Photon. Technol. Lett.*, vol. 17, no. 3, pp. 714–716, Mar. 2005.

[21] M. S. Erkilinc, S. Kilmurray, S. Pachnicke, H. Griesser, B. C. Thomsen, P. Bayvel, and R. I. Killey, "Nyquist-shaped dispersion-precompensated subcarrier modulation with direct detection," presented at the Optical Fiber Communication Conf., San Francisco, CA, USA, Mar. 2014, Paper Th3K.4.

[22] M. S. Erkılınç, S. Pachnicke, H. Griesser, B. C. Thomsen, P. Bayvel, and R. I. Killey, "Effect of clipping on the performance of Nyquist-shaped dispersion-precompensated subcarrier modulation transmission with direct detection," presented at the Eur. Conf. Optical Communication, Cannes, France, Sep. 2014, Paper Tu.3.3.1.

[23] C. R. Berger, Y. Benlachtar, R. I. Killey, and P. A. Milder, "Theoretical and experimental evaluation of clipping and quantization noise for optical OFDM," *Opt. Exp.*, vol. 19, no. 18, pp. 17713–17728, 2011.

[24] R. P. Giddings, X. Q. Jin, E. Hugues-Salas, E. Giacoumidis, J. L. Wei, and J. M. Tang, "Experimental demonstration of a record high 11.25 Gb/s real-time optical OFDM transceiver supporting 25 km SMF end-to-end transmission in simple IMDD systems," *Opt. Exp.*, vol. 18, no. 6, pp. 5541–5555, 2010.

[25] J. M. Cioffi, *Course Notes* [Online]. ch. 4, pp. 317–323, 2013. Available: http://www.stanford.edu/group/cioffi/book

[26] D. Bykhovsky and S. Arnon, "An experimental comparison of different bit-and-power allocation algorithms for DCO-OFDM," *J. Lightw. Technol.*, vol. 32, no. 8, pp. 1559–1564, Apr. 2014.

[27] X. Q. Jin, J. L. Wei, R. P. Giddings, T. Quinlan, S. Walker, and J. M. Tang, "Experimental demonstrations and extensive comparisons of end-to-end real-time optical OFDM transceivers with adaptive bit and/or power loading," *IEEE Photon. J.*, vol. 3, no. 3, pp. 500–511, Jun. 2011.

[28] E. Giacoumidis, A. Kavatzikidis, A. Tsokanos, J. M. Tang, and I. Tomkos, "Adaptive loading algorithms for IMDD optical OFDM PON systems using directly modulated lasers," *J. Opt. Commun. Netw.*, vol. 4, no. 10, pp. 769–778, 2012.

[29] G. P. Agrawal, *Applications of Nonlinear Fiber Optics*, 3rd ed. New York, NY, USA: Academic, 2010.

[30] J.-J. van de Beek, O. Edfors, M. Sandell, S. K. Wilson, P. O. Börjesson, "On channel estimation in OFDM systems," in *Proc. IEEE Veh. Technol. Conf.*, Jul. 1995, vol. 2, pp. 815–819.

[31] N. Liu, X. Chen, C. Ju, and R. Hui, "40-Gbps vestigial sideband half-cycle Nyquist subcarrier modulation transmission experiment and its comparison with orthogonal frequency division multiplexing," *Opt. Eng.*, vol. 53, no. 9, pp. 096114-1–096114-4, 2014.

[32] S. D. Dissanayake and J. Armstrong, "Comparison of ACO-OFDM, DCO-OFDM and ADO-OFDM in IM/DD systems," *J. Lightw. Technol.*, vol. 31, no. 7, pp. 1063–1072, Apr. 2013.

[33] J. L. Wei, D. G. Cunningham, R. V. Penty, and I. H. White, "Study of 100 gigabit ethernet using carrierless amplitude/phase modulation and optical OFDM," *J. Lightw. Technol.*, vol. 31, no. 9, pp. 1367–1373, May 2013.

[34] Z. Li, M. S. Erkilinc, S. Pachnicke, H. Griesser, B. C. Thomsen, P. Bayvel, and R. I. Killey, "Direct-detection 16-QAM Nyquist-shaped subcarrier modulation with SSBI mitigation," in *Proc. IEEE Int. Conf. Commun.*, Jun. 2015, submitted for publication.

M. Sezer Erkılınç (S'11) received the B.Sc. degree in electrical and electronic engineering from Koç University, Istanbul, Turkey, in 2009, and the M.Sc. degree from the Rochester Institute of Technology, Rochester, NY, USA, in 2011. He is currently working toward the Ph.D. degree in optical networks group in the Department of Electronic and Electrical Engineering at the University College London, London, U.K., since November, 2011. He is currently investigating spectrally efficient modulation formats and DSP-based dispersion precompensation techniques for metro/access networks. He is a graduate student member of IEEE and SPIE since 2011.

Stephan Pachnicke (M'09–SM'12) received the M.Sc. degree in information engineering from City University, London, U.K., in 2001, and the Dipl.Ing. and Dr. Ing. degrees in electrical engineering from TU Dortmund, Dortmund, Germany, in 2002 and 2005, respectively. In 2005, he also got the Dipl.-Wirt.-Ing. degree in business administration from Fern Universitt, Hagen, Germany. In January 2012, he finished his habilitation on optical transmission networks and since then he works as a Privatdozent (Adjunct Professor) at TU Dortmund. From 2007 until 2011, he was working as an Oberingenieur at the Chair for High Frequency Technology, TU Dortmund. He is currently with ADVA Optical Networking SE in the Advanced Technology Group (CTO Office), where he is leading EU-funded research projects on next-generation optical access and fixed-mobile convergence. He is an author or coauthor of more than 80 scientific publications as well as the author of a book on Fiber-Optic Transmission Networks (New York, NY, USA: Springer, 2011). He is a Member of VDE/ITG.

Helmut Griesser received the Dipl.Ing. and Dr. Ing. degrees in electrical engineering from the University of Ulm, Ulm, Germany. From 2002 till 2011, he was with Marconi and Ericsson on high-speed fiber transmission. He is a Principal Engineer in the Advanced Technology Group at ADVA Optical Networking, Munich, Germany. His current research interests include signal processing, coding, modulation formats, and system design for optical fiber communication systems.

Benn C. Thomsen (M'06) received the B.Tech. degree in optoelectronics and the M.Sc. and Ph.D. degrees in physics from The University of Auckland, Auckland, New Zealand. His doctoral research involved the development and characterization of short optical pulse sources suitable for high-capacity optical communication systems. He then joined the Optoelectronics Research Centre, Southampton University, Southampton, U.K., as a Research Fellow in 2002, where he carried out research on ultrashort optical pulse generation and characterization, optical packet switching based on optically coded labels, and all-optical pulse processing. He joined the Optical Networks Group, University College London (UCL), London, U.K., in 2004, and held an EPSRC Advanced Fellowship from 2006 to 2011 and was appointed as a Lecturer in 2007. He is currently a Senior Lecturer at UCL and his research interests include optical transmission, physical-layer implementation of dynamic optical networking technology, and the development of high-capacity multimode fiber systems exploiting MIMO DSP.

Polina Bayvel received the B.Sc. (Eng.) and Ph.D. degrees in electronic and electrical engineering from the University of London, London, U.K., in 1986 and 1990, respectively. In 1990, she was with the Fiber Optics Laboratory, General Physics Institute, Moscow (Russian Academy of Sciences), under the Royal Society Postdoctoral Exchange Fellowship. She was a Principal Systems Engineer with STC Submarine Systems, Ltd., London, and Nortel Networks,Harlow, U.K., and Ottawa, ON, Canada, where she was involved in the design and planning of optical fiber transmission networks. During 1994–2004, she held a Royal Society University Research Fellowship at University College London (UCL), and in 2002, she became the Chair in Optical Communications and Networks. She is currently the Head of the Optical Networks Group, UCL. She has authored or coauthored more than 350 refereed journal and conference papers. Her research interests include wavelength-routed optical networks, high-speed optical transmission, and the mitigation of fiber nonlinearities.

She is a Fellow of the Royal Academy of Engineering, the Optical Society of America, the U.K. Institute of Physics, and the Institute of Engineering and Technology. She received the Royal Society Wolfson Research Merit Award from (2007 to 2012), the 2013 IEEE Photonics Society Engineering Achievement Award, and the 2014 Royal Society Clifford Patterson Prize Lecture and Medal.

Robert I. Killey (M'00) received the B.Eng. degree in electronic and communications engineering from the University of Bristol, Bristol, U.K., in 1992, and the M.Sc. degree from University College London (UCL), London, U.K., in 1994, and the D.Phil. degree from the University of Oxford, Oxford, U.K., in 1998. Following this, he joined the Optical Networks Group at UCL where he is currently a Reader in Optical Communications. He serves on the technical program committees of ECOC and OFC conferences, was a Member of the conference committees of ACP, OECC, and IEEE LEOS Annual Meetings, and was the General Cochair of the Signal Processing for Photonic Communications meeting at the OSA Advanced Photonics Congress. He was an Associate Editor of the IEEE/OSA JOURNAL OF OPTICAL COMMUNICATIONS AND NETWORKING. His research interests include nonlinear fiber effects in WDM transmission systems, advanced modulation formats, and digital signal processing for optical communications.